Environmental Science and Pollution Research (2023) 30:6068–6079
https://doi.org/10.1007/s11356-022-22616-6

RESEARCH ARTICLE

New sustainable and robust catalytic supports for palladium nanoparticles generated from chitosan/cellulose film and corn stem biochar

Camila P. Grandini[1] · Cristiane R. Schmitt[1] · Fábio A. Duarte[2] · Diego S. Rosa[1] · Clarissa H. Rosa[1] · Gilber R. Rosa[1]

Received: 20 June 2022 / Accepted: 16 August 2022 / Published online: 20 August 2022

Abstract

The production of sustainable catalytic supports for palladium nanoparticles is always desired, even more so through the recovery of biomass residues. In this sense, two different solids were investigated — chitosan/cellulose film and corn stem biochar — as catalytic supports of palladium nanoparticles. The solids were carefully characterized and tested in the Suzuki-Miyaura reaction, a typical cross-coupling reaction. The developed catalytic systems proved to be efficient and sustainable, promoted the formation of target products very well, and demanded green reactants under environmentally appropriate conditions. With the results shown in the manuscript, it is expected to contribute to the valorization of biomass and agro-industrial residues in the development of new catalysts for the chemical industry.

Keywords Catalytic support · Chitosan/cellulose film · Corn stem biochar · Palladium nanoparticles · Suzuki-Miyaura cross-coupling · Green chemistry

Introduction

In the context of green chemistry, the search for sustainable catalytic systems for cross-coupling reactions is always desired (Wang et al. 2020). High yields (above 90%) of the desired reaction product are good indicators of the efficiency of a catalytic system; however, the working conditions can be harmful to the environment. Typical catalytic systems for cross-coupling reactions employ a metallic catalyst (Pd normally), auxiliary ligand to stabilize the metal, Lewis base to neutralize the system, solvent, inert atmosphere, and heating (Diederich and Meijere 2004; Negishi 2002). Efforts have been reported in order to reduce the amount of catalytically active species in reactions (Roy and Uozumi 2018) or replace it with a more eco-friendly and less expensive metal (Ma et al. 2021); reduce the use of auxiliary ligands (Serrano et al. 2022); employ less toxic solvents (Su et al. 2022) and bases (Long et al. 2019); and make the reaction conditions milder through the use of lower temperatures (close to room temperature) (Ma et al. 2022), microwave heating (Salih 2022), sonication (Wilson et al. 2018), or elimination of the inert atmosphere (Tian et al. 2022). In addition, the search for new, greener catalytic systems employing biomass sources appears frequently in literature, such as in the use of biomass extracts to prepare metal nanoparticles (NPs) via biogenic routes (Schmitt et al. 2021) or green solvents applied in carbon–carbon

Statement of novelty The merit of the manuscript is based on the recovery and reuse of widely available biomass residues through their conversion into catalytic supports for palladium nanoparticles. Thus, two sustainable supports were produced: (i) corn stem biochar and (ii) hybrid polymeric film composed of chitosan and cellulose. Both generated robust and active catalysts in the Suzuki-Miyaura reaction for up to ten successive runs. The catalyst produced using chitosan/cellulose film showed a better performance in the investigation and mechanistic studies indicated that no metal leaching occurs.

Responsible Editor: George Z. Kyzas

✉ Gilber R. Rosa
gilberrosa@furg.br

[1] Escola de Química e Alimentos, Universidade Federal do Rio Grande - FURG, Campus Santo Antônio da Patrulha. Rua Barão do Cahy, 125, Cidade Alta, CEP, Santo Antônio da Patrulha, RS 95500-000, Brazil

[2] Departamento de Química, Universidade Federal de Santa Maria – UFSM, Av. Roraima, 1000, CEP, Santa Maria, RS 97105-900, Brazil

and carbon–heteroatom couplings (Peixoto et al. 2022). On the other hand, biomass material is also used as a catalytic support of active metals, giving rise to efficient catalysts which employ, for example, biochar (Gholinejad et al. 2019), calcined materials (Rosa et al. 2019), or polymeric films (Faria et al. 2014) in cross-coupling reactions. In terms of novel catalytic systems, the Suzuki-Miyaura reaction is commonly preferred because it is one of the most widely studied couplings and because of its importance as a key step in the synthesis of bioactive molecules (Miyaura and Suzuki 1995).

As previously shown, the search for new eco-friendly catalytic systems based on palladium is current and of interest to the chemical industry of organic synthesis; thus, this line of investigation is the main objective of the present manuscript. Focusing on the search for a biomass source capable of being used as a catalytic support in coupling reactions, materials such as chitosan, cellulose, and corn stem have high potential for application given their wide availability and low cost (Kumari and Kishor 2020; Heinze 2016; CONAB 2022). Thus, chitosan (Fig. 1, top), a polysaccharide derived from the deacetylation of chitin, is extremely abundant as it composes the exoskeletons of marine crustaceans, for example (Kumari and Kishor 2020). In this way, the investigation of new uses for chitosan corroborates the fishing industry's need to value its generated waste. Likewise, cellulose (Fig. 1, bottom), an extremely abundant polysaccharide present in plants, stands out for its low cost and wide range of applications (Heinze 2016). And, finally, the corn stem biomass residue includes the prerequisites abundance and low cost, since only Brazil recently had a cereal planted area of 72.9 million hectares in the 2020/2021 harvest (CONAB 2022).

Given this scenario, in this article we report the production of catalytic supports for Pd NPs using raw materials from biomass (chitosan and cellulose) widely available commercially, in addition to an agro-industry residue (corn stem). Emphasizing the use of these low value-added materials will contribute to more sustainable processes since such materials were obtained via simpler routes in terms of unit operations and processing, normally requiring lower energy consumption (Arancon et al. 2013; Maroušek and Trakal 2022). Also, the valorization of biomass corroborates for a better use of residues within its production chain, allowing a greater fixation of income in small producers (Arancon et al. 2013; Maroušek and Trakal 2022). Thus, chitosan/cellulose film (CCF) and corn stem biochar (CSB) were produced and evaluated as catalytic supports for Pd NPs, generating catalysts named Pd/CCF and Pd@CSB, respectively. The solids were tested in the Suzuki-Miyaura cross-coupling, showing efficiency and robustness.

Experimental section

The reagents used in the assays are of analytical purity as the reported work was conducted and tested only at the laboratory bench level.

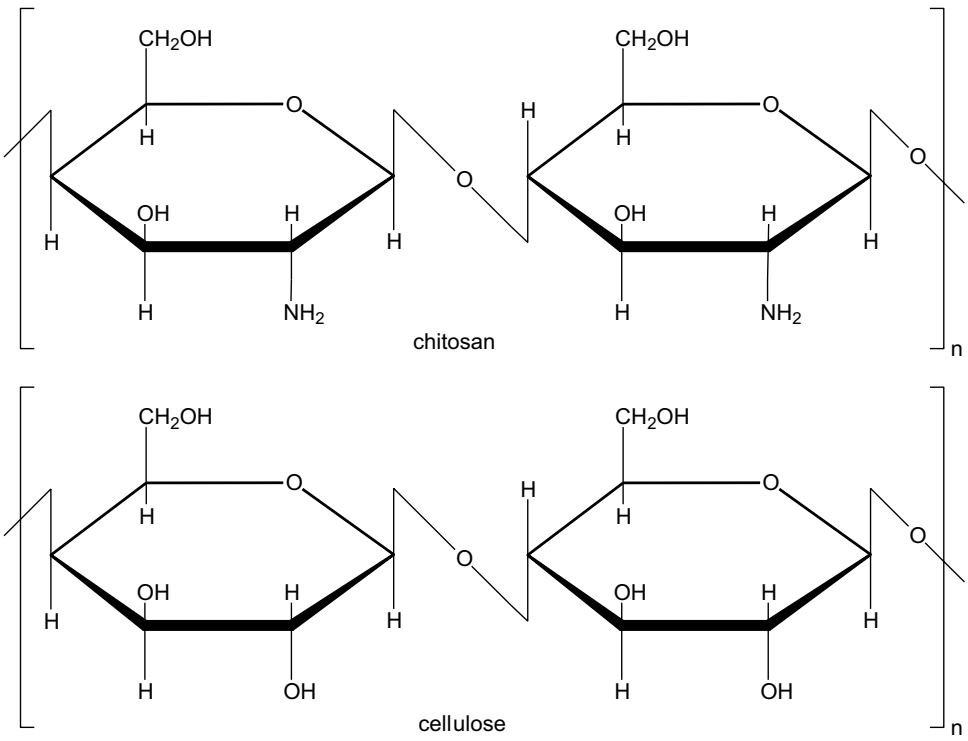

Fig. 1 Chemical structure of chitosan (top) and cellulose (bottom)

Preparation of Pd/CCF catalyst

Initially Pd NPs were obtained by dissolution of 24 mg of palladium (II) chloride ($PdCl_2$; Sigma-Aldrich, 99%) in 10 mL of isopropyl alcohol (C_3H_8O; Proquimios, 99.5%) stirring by 30 min on a stir plate (Ika, model C-MAG HS 7 D). During this process, 1 mL of 0.1 M hydrochloric acid (HCl; Tedia, 37%) was added to dissolve the salt. After fully dissolution, sodium borohydride ($NaBH_4$; Sigma-Aldrich, 99%) reducer solution (53.2 mg in 20 mL of 0.01 M of potassium hydroxide [KOH; Vetec, 85%]) was added and stirred for 1 h until the formation of Pd NPs. Centrifugation step (centrifuge manufactured by Nova Técnica, model NT-825) with isopropyl alcohol washes (3×, 5 min, 3500 rpm) was necessary to Pd NP purification, and finally the solid was dried over laboratory oven (Odontobrás, model EL-1.2 [80 °C, 30 min]). Yield: 11 mg.

Subsequently, the chitosan/cellulose film (CCF) was produced by preparing a solution containing 0.2 g of commercial chitosan (Sigma-Aldrich, deacetylation degree of 75%), 1.7 mL of 1 M acetic acid ($C_2H_4O_2$; Synth, 99.5%), and 10 mL of distilled water, being stirred for 2 h at 60 °C. After the formation of a viscous liquid, a second solution containing microgranular cellulose (Synth, 90% [0.2 g in 10 mL of distilled water]) was added together with 10 mg of previously prepared Pd NPs. Stirring was continued until a homogeneous phase was obtained. The film was produced in a glass Petri plate having a thickness of 20 µm, being left to rest for solvent evaporation (12 h, room temperature). Yield: 789 mg.

Preparation of Pd@CSB catalyst

Corn stem samples were collected in the city of Santo Antônio da Patrulha-RS (Brazil). After manual cutting, washing with deionized water, oven drying (105 °C, 24 h), grounding, and sieving to obtain particle size in the range of 1.68 to 2.00 mm, the samples were carbonized in a muffle furnace (Quimis, model Q318M21 [7 g, 300 °C, 20 min]) yielding 2.59 g of corn stem biochar (CSB). To prepare the catalyst containing Pd NPs, 135 mg of CSB was weighed and 20 mL of a solution containing 25 mg of $PdCl_2$ diluted in isopropanol/water (1:1) was added. The resulting system stayed in an ultrasonic bath (Cole-Parmer, model 08895-31) for 5 min and then the reducing agent was added (26.6 mg of $NaBH_4$ in 10 mL of 0.01 M KOH). Stirring continued for 2 h (room temperature) on a magnetic stirrer (Ika, model C-MAG HS 7 D) and, at the end, the Pd@CSB solid was filtered and oven dried (80 °C, 2 h). Yield: 148 mg of Pd@CSB.

Transmission electron microscopy analysis (TEM)

TEM analyses were performed using a JEOL JEM 1400 operated at 120 kV. The samples were prepared by deposition of the solid from an isopropanol suspension onto a carbon-coated copper grid at room temperature.

Scanning electron microscopy (SEM)

The morphology of the solids was analyzed using a JEOL model JSM 6610 at 20 kV. The samples were gold coated for analysis.

Fourier transform infrared spectroscopy (FT-IR)

FT-IR analyses were conducted using a Shimadzu spectrophotometer, model IR Prestige 21, combining 32 scans at a 2-cm^{-1} resolution. The Pd@CSB sample was analyzed as pellet with an approximate thickness and diameter of 2 mm and 5 mm, respectively. The sample mass dilution was performed with KBr. The Pd/CCF sample was analyzed as a film using direct reading with attenuated total reflectance (ATR) mode after 45 scans.

Porosimetric evaluation (BET isotherms)

N_2 adsorption isotherms were performed on Micrometrics Tristar II 3020 equipment. Initially, samples were preheated at 70 °C for 8 h under vacuum and the surface area was determined using the Brunauer–Emmett–Teller (BET) method at −196 °C with P/P_{atm} in the range of 0.01 to 0.35. The average diameter of mesopores and their distribution were calculated using the Barrett–Joyner–Halenda (BJH) method with Halsey standards for the desorption isotherm. The micropore volume was calculated using the *t*-plot method and the standard isotherm of Harkins and Jura.

Elemental analysis (CHN)

The carbon, hydrogen, and nitrogen compositions (CHN analysis) were performed on a PerkinElmer M-CHNS/O analyzer, model PE 2400 series II.

Inductively coupled plasma optical emission spectrometry (ICP-OES)

A 50 mg sample of the solid Pd@CSB was decomposed using 4 mL of 14.4 mol L^{-1} nitric acid (HNO_3; Qhemis, 65%) and heating to 100 °C (thermostatic bath in Ika apparatus, model C-MAG HS 7 D) and added to 10 mL with ultrapure water. The palladium level was determined (emission line at 340.458 nm) using an inductively coupled plasma optical emission spectrometer (PerkinElmer, model Optima 4300 DV) with an axial view configuration.

Suzuki-Miyaura cross-couplings

Experimental All reactions were conducted under a nitrogen atmosphere in a Schlenk reactor. Bases and solvents

were purchased from Synth (Brazil). Phenylboronic acid (95%) and aryl halides were purchased from Sigma-Aldrich (Brazil). All chemicals were used directly from the original container without prior purification. NMR spectra were recorded on a Bruker Ascend 400-MHz spectrometer. Mass spectra were obtained on a GC/MS PerkinElmer Clarus 600 T (EI, 70 eV) equipped with a 30-m capillary DB-5 column with a dimethylpolysiloxane stationary phase. Gas chromatography was performed on a PerkinElmer Clarus 400 GC equipped with a flame ionization detector (FID) and a 30-m capillary column with a dimethylpolysiloxane stationary phase.

Typical procedure for the Suzuki-Miyaura cross-coupling reaction A Schlenk reactor was charged with base (2 mmol), phenylboronic acid (187 mg, 1.5 mmol), aryl halide (1 mmol), 0.5 mol% of Pd using the catalysts Pd@CSB (5 mg) or Pd/CCF (42 mg), undecane (Sigma-Aldrich, 99% [internal standard, 10 µL]), and solvent (3 mL). The reaction mixture was stirred at 100 °C in a thermostatic oil bath with the aid of a magnetic stir plate (Ika apparatus, model C-MAG HS 7 D). The reaction crude was cooled to room temperature, extracted with 20 mL of diethyl ether ($C_4H_{10}O$; Qhemis, 98%), and washed with 5 mL of sodium hydroxide (NaOH; Synth, 99%) and brine (2 × 5 mL). The organic phase was dried over magnesium sulfate ($MgSO_4$; Synth, 98%), filtered, and concentrated in vacuum; afterward, the crude material was purified by flash chromatography on silica gel (Supelco, pore size 60 Å, 230–400 mesh particle size). The corresponding biaryl products were characterized by ^{1}H and ^{13}C NMR, and by GC-MS.

4-Cyanobiphenyl (Faria et al. 2014). White solid. ^{1}H NMR (400 MHz, $CDCl_3$) δ: 7.72–7.66 (m, 4H), 7.59–7.56 (m, 2H), 7.50–7.39 (m, 3H) ppm. ^{13}C NMR (100 MHz, $CDCl_3$) δ: 145.6, 139.1, 132.5, 129.0, 128.6, 127.7, 127.2, 118.9, 110.8 ppm. GC–MS (IE, 70 eV) *m/z* (%): 179 (100, M+), 178 (25), 151 (17), 180 (14), 76 (14), 89 (11), 177 (8), 152 (8).

Biphenyl (Faria et al. 2014). White solid. ^{1}H NMR (400 MHz, $CDCl_3$) δ: 7.59–7.57 (m, 4H), 7.44–7.40 (m, 4H), 7.34–7.31 (m, 2H) ppm. ^{13}C NMR (100 MHz, $CDCl_3$) δ: 141.2, 128.7, 127.2, 127.1 ppm. GC–MS (IE, 70 eV) *m/z* (%): 154 (100, M+), 153 (43), 152 (29), 76 (19), 155 (12), 151 (9), 77 (9), 115 (7).

4-Methylbiphenyl (Faria et al. 2014). White solid. ^{1}H NMR (400 MHz, $CDCl_3$) δ: 7.58–7.56 (m, 2H), 7.48 (d, J = 8.1 Hz, 2H), 7.42–7.39 (m, 2H), 7.32–7.28 (m, 1H), 7.23 (d, J = 7.8 Hz, 2H), 2.38 (s, 3H) ppm. ^{13}C NMR (100 MHz, $CDCl_3$) δ: 141.1, 138.3, 137.0, 129.4, 128.7, 127.0, 126.9, 21.1 ppm. GC–MS (IE, 70 eV) *m/z* (%): 168 (100, M+), 167 (75), 165 (30), 152 (27), 153 (19), 83 (19), 82 (17), 169 (12).

4-Methoxybiphenyl (Faria et al. 2014). White solid. ^{1}H NMR (400 MHz, $CDCl_3$) δ: 7.56–7.51 (m, 4H), 7.43–7.39 (m, 2H), 7.31–7.28 (m, 1H), 6.97 (d, J = 8.8 Hz, 2H), 3.84 (s, 3H) ppm. ^{13}C NMR (100 MHz, $CDCl_3$) δ: 159.1, 140.8, 133.8, 128.7, 128.1, 126.7, 126.6, 114.2, 55.3 ppm. GC–MS (IE, 70 eV) *m/z* (%): 184 (100, M+), 141 (69), 169 (68), 115 (53), 139 (19), 185 (17), 76 (13), 63 (12).

Results and discussion

Chitosan/cellulose film (CCF)

The preparation of palladium nanoparticles (Pd NPs) was carried out as described in the "Experimental section" prior to the production of CCF. Thus, a solution of $PdCl_2$ in isopropyl alcohol was subjected to the $NaBH_4$ reducer until a visible change of color (orange to black) by the formation of Pd NPs. Afterward, the system was washed with isopropyl alcohol, centrifuged, and the Pd NPs were isolated and dried. The size of the nanoparticles was assessed by transmission electron microscopy (Fig. 2).

Figure 2 indicates that the Pd NPs produced had a diameter compatible with other similar reports (Faria et al. 2014). Thus, the preparation of the catalyst continued with the addition of a mixture of Pd NPs, microgranular cellulose, and water in a viscous chitosan solution previously prepared (see "Experimental section"). After homogenization, the liquid was poured into a glass plate for evaporation of the solvent and formation of the film, which was named as Pd/CCF.

A SEM micrograph of Pd/CCF is shown in Fig. 3 (left). The film appeared to have a fibrous structure. EDS analysis of the Pd/CCF (Fig. 3, right) indicated the presence of palladium metal.

Following the investigation, the FT-IR analysis was conducted to assess the presence of organic groups on the Pd/CCF surface (Fig. 4).

In Fig. 4 it is possible to observe characteristic bands of chitosan (Dotto et al. 2013) and cellulose (Fonseca et al. 2020) existing in the Pd/CCF. The existing broad band at 3257 cm^{-1} is associated with O–H and N–H groups. In the range of 2925–2849 cm^{-1}, elongation interactions of the C–H bond can be observed. The signal corresponding to the stretching of the carbonyl is evidenced at 1643 cm^{-1}. The bands located at 1555 cm^{-1} and 1067 cm^{-1} can be associated with elongation of the C–N bond. The signals observed in the region of 1370 cm^{-1} refer to CH_2. And, finally, the band in the region of 1011 cm^{-1} can be associated with the C–O elongation.

Corn stem biochar (CSB)

Initially, corn stalks were collected from rural properties in the city of Santo Antônio da Patrulha-RS (Brazil). After

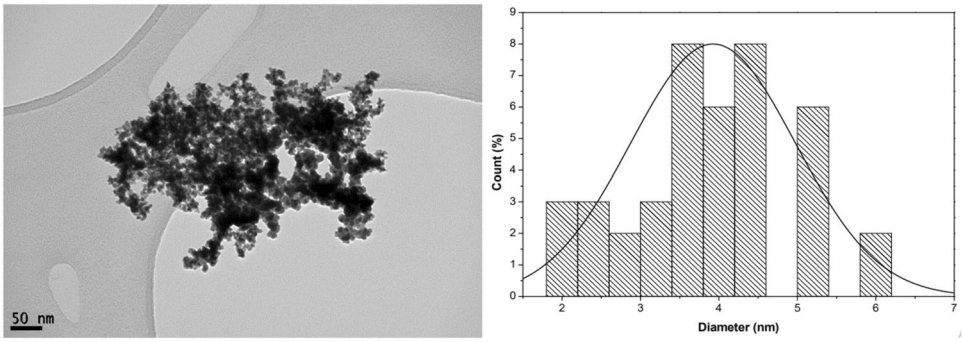

Fig. 2 TEM micrograph of the Pd NPs (left) and a histogram (right) illustrating the particle size distribution

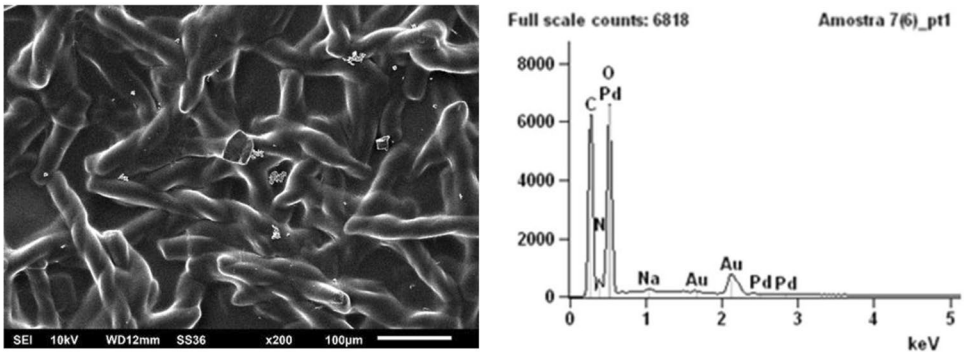

Fig. 3 SEM micrograph illustrating the fibrous surface of Pd/CCF (left) and an EDS pattern showing the detection of Pd metal (right)

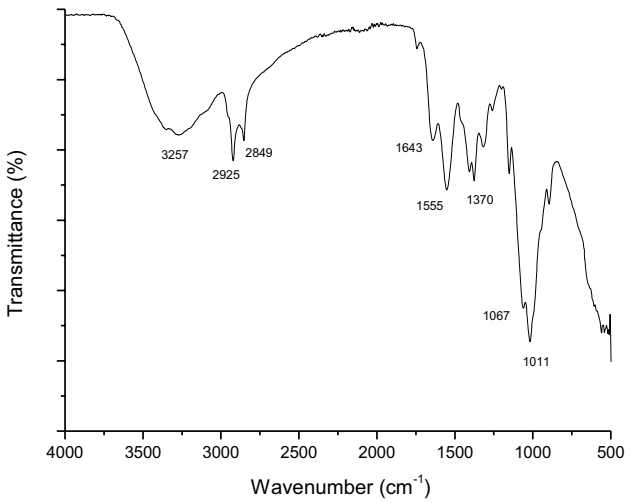

Fig. 4 FT-IR spectrum of Pd/CCF catalyst showing the presence of organic groups on its surface

manual cutting, washing, drying in an oven, and sieving, the samples were carbonized as described in the "Experimental section." Porosimetric (BET isotherms) and CHN analyses were performed on the solids corn stem biochar (CSB) and commercial activated carbon (CAC; Sigma-Aldrich activated carbon #242276) to compare surface properties (Table 1).

Table 1 shows that the surface area of the CAC was about 126× greater than of CSB (entries 1 and 2). This result was expected since the CSB did not undergo an activation process. By analyzing the pore volume, the same tendency was observed; that is, CAC had a pore volume about 411× greater than CSB (entries 1 and 2). In the CHN analysis, it was seen that CSB had a lower percentage of C than CAC due to the heterogeneous composition (see EDS analysis).

For Pd NPs impregnation into the CSB was mixed and stirred (sonication) with $PdCl_2$ solution in isopropanol/water (1:1) for 5 min. After, addition of reducer ($NaBH_4$ in basic solution) was performed to form the Pd(0) NPs. Stirring

Table 1 Surface areas and CHN analysis of CSB and CAC

Entry	Sample	Specific Area ($m^2\ g^{-1}$)	Micropore volume ($cm^3\ g^{-1}$)	C (%)	H (%)	N (%)
1	CSB	6.26	0.00074	59.37	3.85	0.85
2	CAC	792.83	0.30545	77.47	0.73	0.34

was carried out for 120 min at room temperature. Finally, the resulting solid was filtered, oven dried, and named Pd@CSB. This material was characterized by SEM-EDS, TEM, ICP-OES, and FT-IR analyses.

A SEM micrograph of Pd@CSB solid is shown in Fig. 5 (left). The Pd@CSB solid appeared to have a fibrous structure. EDS analysis of the Pd@CSB (Fig. 5, right) indicated the presence of palladium metal.

TEM analysis was also performed on the prepared Pd@CSB solid; thus, Pd(0) NPs can be encountered as irregular-shaped structures, with a predominant size of 10 nm (Fig. 6).

ICP-OES analysis was performed on the prepared Pd@CSB sample. The Pd loading encountered was 106,476 ± 264 mg kg^{-1} (~0.01% Pd by weight) and this data served as a parameter for determining the Pd@CSB weight used in the catalytic tests.

FT-IR analysis was conducted on the Pd@CSB solid in order to obtain information about the existence of functional groups. The result found is shown in Fig. 7.

In Fig. 7, a characteristic band corresponding to the stretching vibration of −OH groups is evidenced by the broad band near 3340 cm^{-1}. This stretching is attributed to the hydroxyl groups of cellulose, hemicellulose, and lignin present in the CSB, or by the presence of water in the material. Evidence of C–H stretching of alkyl groups of cellulose, hemicellulose, and lignin can also be observed by the peak at around 2905 cm^{-1}. The carbonyl band observed at 1730 cm^{-1} is likely derived from ester groups of hemicellulose or

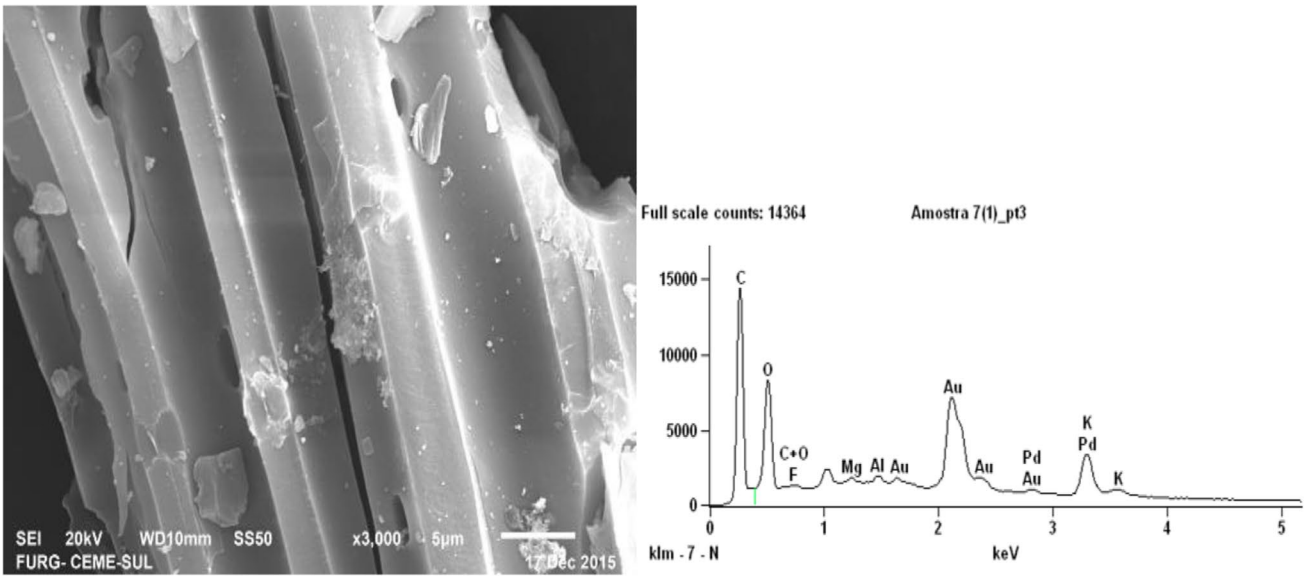

Fig. 5 SEM micrograph illustrating the fibrous structure of Pd@CSB (left) and an EDS pattern showing the detection of Pd metal (right)

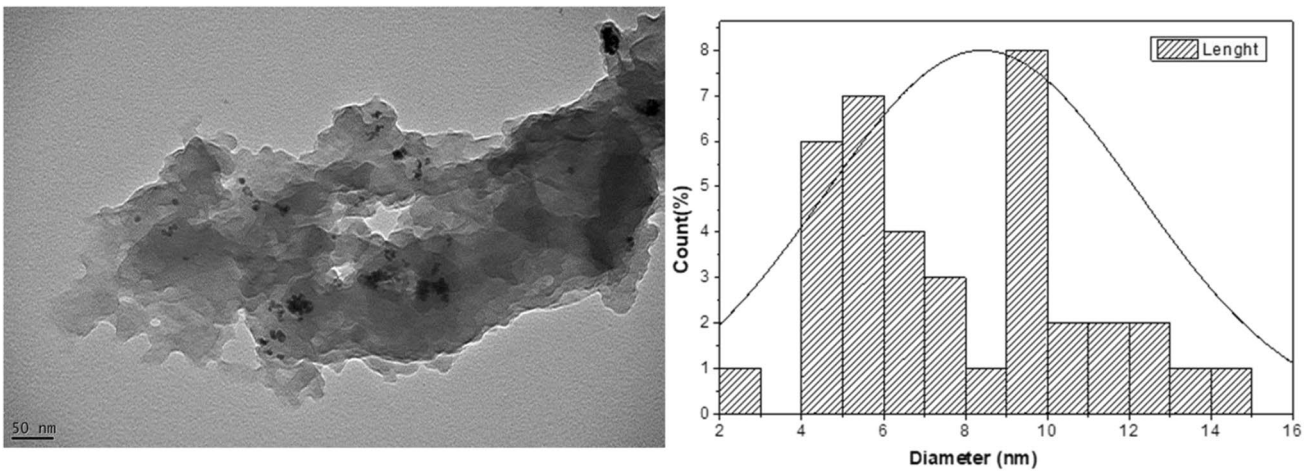

Fig. 6 TEM micrograph of the Pd@CSB indicating Pd(0) NPs (left) and a histogram (right) illustrating the particle size distribution

lignin monomers. The presence of a band at approximately 1604 cm^{-1} may be due to the C–C bond stretching of the aromatic ring of the lignin or to the C=O group, corresponding to the carbonyl of aldehydes and ketones originating from lignin (Farinella et al. 2008). The band at 1239 cm^{-1} corresponds to =C–O–C, which is commonly observed when =C–O– in ether, ester, and phenol groups are present. Finally, the band near 1032 cm^{-1} may be assigned to the (C–O)–C bond stretching of cellulose present in the template structure (Fonseca et al. 2020).

Catalytic tests

Having both solids (Pd/CCF and Pd@CSB) characterized, the Suzuki-Miyaura reaction between phenylboronic acid and 4-bromobenzonitrile was chosen to optimize the catalytic systems (Scheme 1; Table 2). For this purpose, bases and solvents were varied based on previous works of our research group and the use of the eco-friendly reagents was prioritized (Faria et al. 2014; Rosa et al. 2019; Schmitt et al. 2021).

The results presented in Table 2 show that both developed catalysts were successful in the studied reaction (entries 7 and 8), characterizing sustainable catalytic systems as they do not require phosphine ligands and/or quaternary ammonium salts, in addition to employing eco-friendly reagents (ethanol and K_2CO_3). In this sense, the pair K_2CO_3/ethanol (base/solvent) proved to be the most efficient in terms of reaction yield, corroborating previous works by our research group (Rosa et al. 2019; Schmitt et al. 2021). On the other hand, the nonpolar solvent dioxane and the organic base NEt_3 did not provide the maximum catalytic activity of the catalysts tested (entries 1–6). The effect of the catalytic supports (CCF and CSB) on the reaction yield is evident when the reaction under study is repeated only with the Pd NPs (entry 9), indicating the superiority of the Pd/CCF catalyst (entry 7). And obviously, the Suzuki-Miyaura cross-coupling does not occur without the presence of Pd, confirming the real function of the catalysts reported here (entry 10).

With the actual knowledge about the composition of the catalysts, the scope of its use in the Suzuki-Miyaura reaction was increased by varying aryl halides and/or functional groups on the aromatic ring (Table 3).

Table 3 shows the efficiency of the catalysts in the Suzuki-Miyaura cross-coupling without auxiliary ligands. Excellent yields for the coupling of aryl iodides were observed using both catalysts (entries 1–6); however, Pd@CSB needed shorter reaction times than Pd/CCF for the same reactions. Even using electron-donating ArI, the catalysts showed high efficiency in the cross-coupling (entries 3–6). However, using ArBr as cross-coupling partner, Pd@CSB presents intolerance in aryl bromides containing electron donating groups in *para* position (entries 9–12). In general, reaction times increased significantly (to 24 h) due to the difficulty of promoting the first stage of the catalytic cycle (oxidative addition) when ArBr is used.

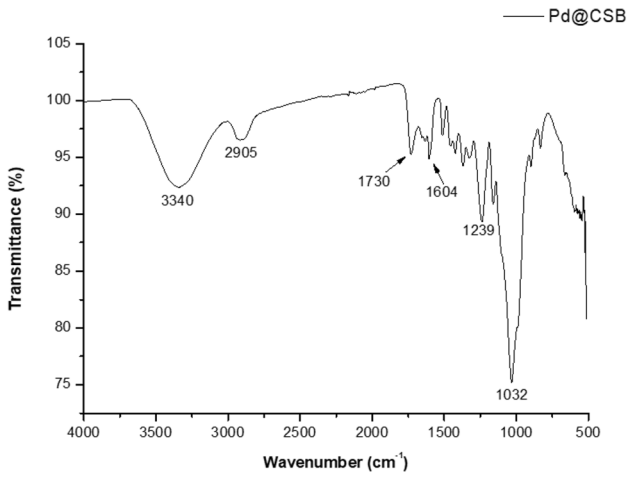

Fig. 7 FT-IR spectrum of Pd@CSB catalyst showing the presence of organic groups on its surface

Table 2 Optimization of reaction conditions for the Suzuki-Miyaura cross-coupling of Pd/CCF and Pd@CSB with phenylboronic acid and 4-bromobenzonitrile[a]

Entry	Solvent	Base	Catalyst	Yield (%)
1	Dioxane	NEt_3	Pd/CCF	41
2	Dioxane	NEt_3	Pd@CSB	36
3	Dioxane	K_2CO_3	Pd/CCF	47
4	Dioxane	K_2CO_3	Pd@CSB	51
5	Ethanol	NEt_3	Pd/CCF	68
6	Ethanol	NEt_3	Pd@CSB	56
7	Ethanol	K_2CO_3	Pd/CCF	99 (95)
8	Ethanol	K_2CO_3	Pd@CSB	89
9	Ethanol	K_2CO_3	Only Pd NPs	70
10	Ethanol	K_2CO_3	No catalyst	0

[a]Reaction conditions: 4-bromobenzonitrile (1 mmol), phenylboronic acid (1.5 mmol), catalyst containing 0.5 mol% of Pd (42 mg of PdCCF or 5 mg of Pd@CSB), base (2 mmol), solvent (3 mL), undecane (10 µL), 20 h, 100 °C, yields determined by GC (average of two runs). The isolated yield is stated in the parentheses

Scheme 1 The Suzuki-Miyaura cross-coupling reaction investigated in this study

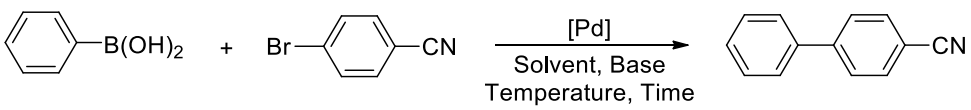

Both catalysts did not tolerate ArCl as cross-coupling partner in the Suzuki-Miyaura reaction (entries 13–18): even employing activated aryl chloride (containing NO_2 group) the reaction yield stayed in order of traces (entries 13 and 14). The other aryl chlorides tested showed no reaction (entries 16–18) but, surprisingly, Pd/CCF promoted the reaction of PhCl in low yield (entry 15). Although the result is minimal, biphenyl was obtained by direct reaction and no evidence of homocoupling of $PhB(OH)_2$ was encountered. In this study, TON and TOF values were calculated and the Pd@CSB catalyst proved to be superior in terms of TOF values (see entries 4 and 6) to other catalytic systems that employ similar conditions (conventional heating and the same amount of catalyst) (Faria et al. 2014; Rosa et al. 2019; Schmitt et al. 2021).

In order to compare the results obtained in Table 3 with other studies using Pd NPs as a catalyst, the Suzuki-Miyaura reaction of 4-bromoanisole with phenylboronic acid was chosen. Thus, Table 4 shows different catalytic systems developed with their particularities.

The best result shown in Table 4 (entry 1) combines a low amount of Pd (0.1 mol%) with a high yield of 4-methoxylbiphenyl (96%) through the use of nanostructured hafnium (IV) oxide as a catalytic support (Wu et al. 2022). The same cross-coupling product yield was obtained by the Pd/CCF catalyst described in the present manuscript employing a higher amount of Pd (entry 7). Identical results in terms of 4-methoxybiphenyl yield were found using cellulose acetate thin film (Faria et al. 2014), soil-derived humic acid-coated iron oxide NPs (Chinchole et al. 2019), and dendritic structure (Sheikh et al. 2022) as catalytic supports of Pd NPs (entries 4, 8, 9). On the other hand, very interesting results are reported employing Pd NP biosynthesis through plant extracts (entries 2, 3, 5). In these reports, it is observed that organic residues from the plant extract remain together with the Pd NPs after their isolation, providing stability to the catalyst in the same way as the catalytic support (Lebaschi et al. 2017; Hekmati et al. 2017; Schmitt et al. 2021). However, the recycling of catalysts containing Pd NPs from biosynthesis is normally less (3–6 runs) than when using a more robust catalytic support (Lebaschi et al. 2017; Hekmati et al. 2017; Schmitt et al. 2021). Obviously, each catalytic system has its pros and cons due to the large number of items that must be observed. Thus, focusing on the results here presented, it can be said that the catalysts reported in this manuscript are among those with potential technological use due to their simplified, eco-friendly, and low-cost production routes.

The term low cost used in the designation of the catalysts produced is justified by the low acquisition value of the materials that were used in the preparation of the Pd NP supports, as well as by the ease of obtaining them. In order to exemplify this fact, the acquisition cost of the main reagents (chitosan, cellulose, and $PdCl_2$) for the production of 1 g of the Pd/CCF catalyst, based on the prices stipulated in Brazil via the suppliers' websites, was USD 5.58. This

Table 3 Suzuki-Miyaura cross-coupling of phenylboronic acid with different aryl halides catalyzed by Pd/CCF and Pd@CSB[a]

Entry	ArX	Catalyst	Time (h)	Yield (%)	TON	TOF
1	PhI	Pd/CCF	5	97	194	39
2	PhI	Pd@CSB	1	99	198	198
3	4-MeC_6H_4I	Pd/CCF	5	98	196	39
4	4-MeC_6H_4I	Pd@CSB	1	97	194	194
5	4-$MeOC_6H_4I$	Pd/CCF	5	98	196	39
6	4-$MeOC_6H_4I$	Pd@CSB	1	95	190	190
7	PhBr	Pd/CCF	24	89	178	7
8	PhBr	Pd@CSB	24	92	184	8
9	4-MeC_6H_4Br	Pd/CCF	24	84	168	7
10	4-MeC_6H_4Br	Pd@CSB	24	80	160	7
11	4-$MeOC_6H_4Br$	Pd/CCF	24	96	192	8
12	4-$MeOC_6H_4Br$	Pd@CSB	24	78	156	6
13	4-$O_2NC_6H_4Cl$	Pd/CCF	36	Traces	---	---
14	4-$O_2NC_6H_4Cl$	Pd@CSB	36	Traces	---	---
15	PhCl	Pd/CCF	36	9	18	0.5
16	PhCl	Pd@CSB	36	NR	---	---
17	4-$MeOC_6H_4Cl$	Pd/CCF	36	NR	---	---
18	4-$MeOC_6H_4Cl$	Pd@CSB	36	NR	---	---

[a]Reaction conditions: ArX (1 mmol), phenylboronic acid (1.5 mmol), catalyst containing 0.5 mol% of Pd (42 mg of Pd/CCF or 5 mg of Pd@CSB), K_2CO_3 (2 mmol), ethanol (3 mL), 100 °C, isolated yields (average of two runs). Time not optimized. *TON* turnover number, yield of product/per mol of Pd. *TOF* turnover frequency, TON/time of reaction (h)

Table 4 Suzuki-Miyaura cross-couplings between phenylboronic acid and 4-bromoanisole by different catalysts containing Pd NPs

Entry	Catalytic support	Pd (mol%)	Yield (%)	Reference
1	Nanostructured hafnium (IV) oxide	0.1	96	Wu et al. (2022)
2	No support. Pd NP biosynthesis by black tea leaves (*Camellia sinensis*) extract	0.1	96	Lebaschi et al. (2017)
3	No support. Pd NP biosynthesis by *Hibiscus sabdariffa* L. flower extract	0.2	85	Hekmati et al. (2017)
4	Dendritic structure	0.47	90	Sheikh et al. (2022)
5	No support. Pd NP biosynthesis by yerba mate aqueous extract	0.5	91	Schmitt et al. (2021)
6	Corn stem biochar	0.5	78	This work
7	Chitosan/cellulose film	0.5	96	This work
8	Soil-derived humic acid-coated iron-oxide NPs	0.65	90	Chinchole et al. (2019)
9	Cellulose acetate thin film	1.0	90	Faria et al. (2014)

value is quite low compared to the most popular Pd catalyst, tetrakis (triphenylphosphine)palladium(0) (Negishi 2002), used in Suzuki-Miyaura cross-coupling, which costs about USD 89.40 per gram (Sigma-Aldrich 2022).

In this same approach, the effect of the COVID-19 pandemic on the prices of less noble metals such as copper, aluminum, zinc, and silver is observed (Vochozka et al. 2021; Rowland et al. 2022; Novakova et al. 2022; Bartos et al. 2022). Obviously, nobler metals like palladium also experienced an increase in their commercial value due to this same cause. Thus, it is interesting to think about the economic reality when developing technological products derived from these metals. And, in this sense, the catalytic systems reported in the present manuscript are in line with this trend since they employ an adequate palladium load (0.5 mol%) and provide a very good to high yield of product (78–96%) according to Table 4 (entries 6 and 7).

The recycle of the catalysts under study were carry out by choosing the reaction of 4-iodoanisole with phenylboronic acid to analyze this parameter (Table 3, entries 5 and 6). For Pd/CCF was used reaction time of 5 h and, for Pd@CSB, the reaction time was of 1 h as is shown in Table 3 (entries 5 and 6). In this way, in the first run, 98% yield was obtained within Pd/CCF and 95% yield with Pd@CSB. After first run, the reaction crude was filtered and the solid (catalyst and K_2CO_3) was washed with ethanol and returned to Schlenk reactor to another run. The same procedure was repeated in the other runs. The performance of the catalysts in the recycling study can be seen in Fig. 8.

As shown in Fig. 8, Pd/CCF showed excellent catalytic activity during ten successive runs. The tests stopped in tenth run because the film was disintegrating. On the contrary, Pd@CSB showed to lost catalytic activity during recycle, showing very good yield (~80%) until the fifth run. Anyway, both catalysts were actives during 10 runs and this fact represents the robustness of the catalytic precursors developed.

As Pd/CCF catalyst have shown interesting performance in recycling study, further investigations were conducted to clarify the catalytically active Pd species involved. In this sense, an important tool to assess Pd leaching is the hot filtration test (Phan et al. 2006; Rosa et al. 2019). In general, the test consists of filtering the reaction mixture while it is still hot in order to separate the added catalyst (solid) from the reaction medium, which is subsequently heated again. Finally, it is evaluated whether there was an increase in the product yield in the absence of the catalyst. If this occurs, there is evidence of Pd soluble and active in the system. In the investigation conducted with Pd/CCF, the reaction chosen was that of 4-iodoanisole with phenylboronic acid (Table 3, entry 5). This reaction generated 70% of the respective biphenyl (monitored via GC) in a time of 1 h (100 °C). Thus, after 1 h of reaction, the reaction crude was filtered through a heated filtration system, and the filtrate was again taken to a new reactor. The system was heated and stirred for another 4 h under the same usual reaction conditions. Finally, the reaction crude was read again via GC and no significant increase in the amount of the respective biphenyl was evidenced. The comparison of the results obtained with and without Pd/CCF catalyst proved that the evolution of the reaction yield is totally inhibited after removing the catalytic precursor from the reaction medium. These data indicate that the active Pd remains in the Pd/CCF and, thus, it can be inferred that the reaction is promoted on the surface of the CCF in the case of heterogeneous catalysis.

Assessment of the homogeneous or heterogeneous nature of the active Pd species continued with the metallic mercury poisoning test (Phan et al. 2006; Baran et al. 2015; Rosa et al. 2019). Such an assay, when effective, inhibits the catalytic activity of the metal under analysis due to the formation of an alloy (amalgam) with Hg, resulting in a catalytically inactive material. This fact is an indication that catalytically active Pd(0) is present in the catalytic cycle. On the other hand, if the addition of metallic mercury does not influence the catalytic activity, it may be possible to have a catalyst that does not include unprotected Pd(0) supported or in solution in the reaction medium (Phan et al. 2006). Based on this information, the reaction between phenylboronic acid and

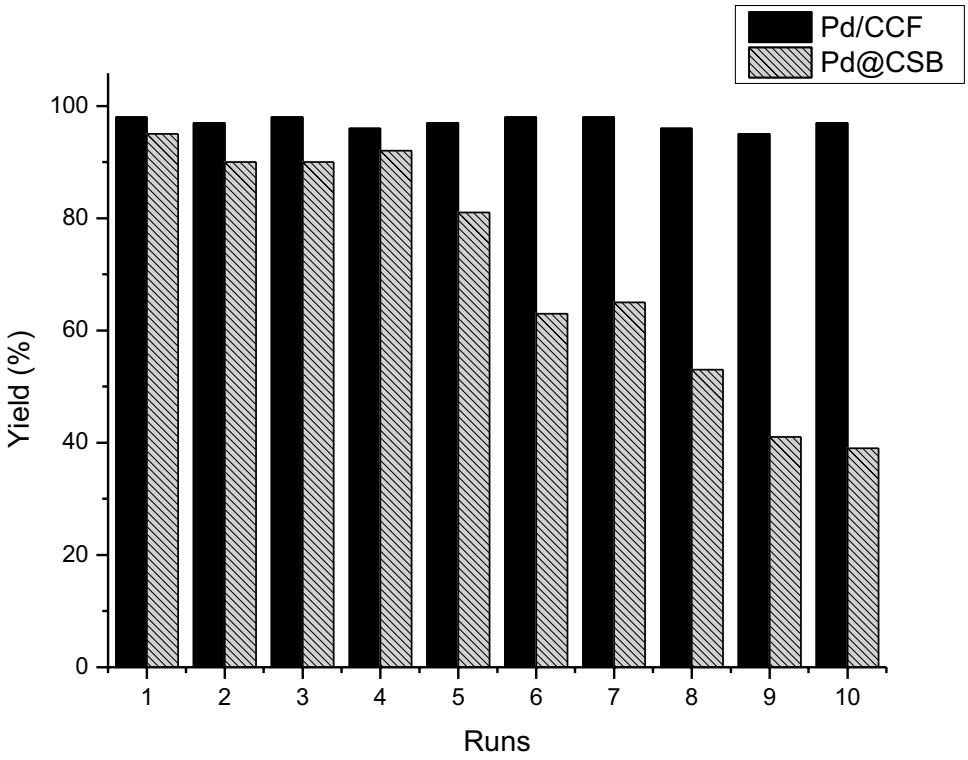

Fig. 8 Recycle of Pd/CCF and Pd@CSB catalysts in repeated runs of the Suzuki-Miyaura cross-coupling of phenylboronic acid with 4-iodoanisole

4-iodoanisole was chosen (Table 3, entry 5), with 0.2 mmol of Hg(0) being added to the reactor concomitantly with the reagents. After 5 h of reaction, GC analysis showed that only 16% of the product (4-methoxybiphenyl) was formed, also indicating traces of biphenyl, which is the by-product from the homocoupling of phenylboronic acid. It is important to remember that in the absence of Hg(0) the same reaction had a yield of 98%.

In a second Hg(0) poisoning study, the same reaction started like as usual (Table 3, entry 5) but, after 1 h, 0.2 mmol de Hg(0) was added and the stirring continued until complete 5 h. Again, the appearance of reaction by-products was observed. An aliquot for GC analysis was removed before Hg(0) was added (reaction time of 1 h) and indicated a 55% yield of 4-methoxybiphenyl. This value did not change after the addition of Hg(0).

In summary, it can be said that the results of hot filtration and Hg(0) poisoning tests together indicate that the real catalytic species is unprotected Pd(0) and supported in CCF.

Conclusion

In conclusion, in this work two catalysts were produced containing Pd NPs and using easy-to-prepare catalytic supports from chitosan, cellulose, and corn stem. Such solids were properly characterized and tested in the Suzuki-Miyaura reaction, showing interesting catalytic activity. The catalytic systems reported can be characterized as sustainable due to the fact that they use eco-friendly reagents, do not use toxic auxiliary ligands, in addition to demonstrating excellent catalyst recyclability. It is believed that both catalysts have technological appeal given the simplicity of obtaining them, robustness, and low cost in the acquisition of their raw materials. Focusing on cost and comparing the mass of 1 g, the reagents needed for the production of the Pd/CCF catalyst cost about 6% of the value of the best-selling Pd-based catalyst, tetrakis (triphenylphosphine)palladium(0). Thus, our group believes in the potential of the catalysts reported here and continues their study seeking the development of new applications in cross-coupling reactions (mainly Heck-Mizoroki and Sonogashira). Also, with the results presented in the manuscript, it is expected to add value to biomass and agro-industrial residues, contributing to the state of the art in the development of new catalysts for the chemical industry.

Supplementary Information The online version contains supplementary material available at https://doi.org/10.1007/s11356-022-22616-6.

Author contribution All authors contributed to the study conception and design. Material preparation, data collection, and analysis were performed by Camila P. Grandini, Cristiane R. Schmitt, Fábio A. Duarte, and Diego S. Rosa. The first draft of the manuscript was written by Clarissa H. Rosa and Gilber R. Rosa, and all authors commented on previous versions of the manuscript. All authors read and approved the final manuscript.

Funding This work was supported by grants from CNPq and FAPERGS (edital FAPERGS/CNPq 12/2014 – PRONEX, protocol 18795.341.30460.15012015), Brazil.

Data availability All data generated or analyzed during this study are included in this published article and its supplementary information files. Supplementary data (copies of NMR) mentioned in the manuscript are available free of charge as PDF file.

Declarations

Ethics approval and consent to participate Not applicable.

Consent for publication Not applicable.

Competing interests The authors declare no competing interests.

References

Arancon RAD, Lin CSK, Chan KM et al (2013) Advances on waste valorization: new horizons for a more sustainable society. Energy Sci Eng 1:53–71. https://doi.org/10.1002/ese3.9

Baran T, Açıksöz E, Menteş A (2015) Carboxymethyl chitosan Schiff base supported heterogeneous palladium(II) catalysts for Suzuki cross-coupling reaction. J Mol Catal A-Chem 407:47–52. https://doi.org/10.1016/j.molcata.2015.06.008

Bartos V, Vochozka M, Šanderova V (2022) Copper and aluminium as economically imperfect substitutes, production and price development. Acta Montan Slovaca: 462–478. https://doi.org/10.46544/AMS.v27i2.14

Chinchole AN, Dubey AV, Kumar AV (2019) Bioinspired palladium nanoparticles supported on soil-derived humic acid coated iron-oxide nanoparticles as catalyst for C–C cross-coupling and reduction reactions. Catal Lett 149:1224–1236. https://doi.org/10.1007/s10562-019-02703-z

CONAB (2022) Companhia Nacional de Abastecimento – Brazil (National Supply Company). National grain production is estimated at 269.3 million tons in the 2021/22 harvest. https://cast.conab.gov.br/post/2022-04-07_7_bol_safras/. Accessed 29 May 2022 (in Portuguese)

Diederich F, Meijere A (2004) Metal-catalyzed cross-coupling reactions, 2nd edn. Wiley-VCHVerlag GmbH&Co, Weinheim

Dotto GL, Moura JM, Cadaval TRS, Pinto LAA (2013) Application of chitosan films for the removal of food dyes from aqueous solutions by adsorption. Chem Eng J 214:8–16. https://doi.org/10.1016/j.cej.2012.10.027

Faria VW, Oliveira DGM, Kurz MHS et al (2014) Palladium nanoparticles supported in a polymeric membrane: an efficient phosphine-free "green" catalyst for Suzuki–Miyaura reactions in water. RSC Adv 4:13446–13452. https://doi.org/10.1039/C4RA01104J

Farinella NV, Matos GD, Lehmann EL, Arruda MAZ (2008) Grape bagasse as an alternative natural adsorbent of cadmium and lead for effluent treatment. J Hazard Mater 154:1007–1012. https://doi.org/10.1016/j.jhazmat.2007.11.005

Fonseca CS, Rosa CH, Lopes TJ, Rosa GR (2020) Sewage sludge in phenol and methylene blue adsorption: a miniproject for teaching sustainability. J Chem Educ 97:1087–1092. https://doi.org/10.1021/acs.jchemed.9b01118

Gholinejad M, Naghshbandi Z, Nájera C (2019) Carbon-derived supports for palladium nanoparticles as catalysts for carbon-carbon bonds formation. ChemCatChem 11:1792–1823. https://doi.org/10.1002/cctc.201802101

Heinze T (2016) Cellulose: Structure and Properties. In: Rojas OJ (ed) Cellulose chemistry and properties: fibers, nanocelluloses and advanced materials, 1st edn. Springer International Publishing, Cham, pp 1–52

Hekmati M, Bonyasi F, Javaheri H, Hemmati S (2017) Green synthesis of palladium nanoparticles using *Hibiscus sabdariffa* L. flower extract: heterogeneous and reusable nanocatalyst in Suzuki coupling reactions. Appl Organomet Chem 31:e3757. https://doi.org/10.1002/aoc.3757

Kumari S, Kishor R (2020) Chitin and chitosan: origin, properties, and applications. In: Gopi S, Thomas S, Pius A (eds) Handbook of Chitin and Chitosan, 1st edn. Elsevier, Amsterdam, pp 1–33

Lebaschi S, Hekmati M, Veisi H (2017) Green synthesis of palladium nanoparticles mediated by black tea leaves (*Camellia sinensis*) extract: catalytic activity in the reduction of 4-nitrophenol and Suzuki-Miyaura coupling reaction under ligand-free conditions. J Colloid Interface Sci 485:223–231. https://doi.org/10.1016/j.jcis.2016.09.027

Long B-F, Qin G-F, Huang Q et al (2019) Homocoupling of arylboronic acids catalyzed by dinuclear copper(I) complexes under mild conditions. J Iran Chem Soc 16:2639–2646. https://doi.org/10.1007/s13738-019-01728-w

Ma X, Wang H, Liu Y et al (2021) Mixed alkyl/aryl diphos ligands for iron-catalyzed Negishi and Kumada cross coupling towards the synthesis of diarylmethane. ChemCatChem 13:5134–5140. https://doi.org/10.1002/cctc.202101237

Ma B, Shi Q, Ma X et al (2022) Defect-free alternating conjugated polymers enabled by room-temperature Stille polymerization. Angew Chem Int Edit 61:e202115969. https://doi.org/10.1002/anie.202115969

Maroušek J, Trakal L (2022) Techno-economic analysis reveals the untapped potential of wood biochar. Chemosphere 291:133000. https://doi.org/10.1016/j.chemosphere.2021.133000

Miyaura N, Suzuki A (1995) Palladium-catalyzed cross-coupling reactions of organoboron compounds. Chem Rev 95:2457–2483. https://doi.org/10.1021/cr00039a007

Negishi E (ed) (2002) Handbook of organopalladium chemistry for organic synthesis. John Wiley & Sons, Inc, New York

Novakova L, Novotna L, Prochazkova M (2022) Predicted future development of imperfect complementary goods — copper and zinc until 2030. Acta Montan Slovaca: 135, https://doi.org/10.46544/AMS.v27i1.10-151

Peixoto MLB, Silva CHL, Godoi M (2022) Generation of new carbon–carbon and carbon–heteroatom bonds mediated by agro-waste extracts: a review. Environ Chem Lett 20:841–873. https://doi.org/10.1007/s10311-021-01343-3

Phan NTS, Van Der Sluys M, Jones CW (2006) On the nature of the active species in palladium catalyzed Mizoroki–Heck and Suzuki–Miyaura couplings — homogeneous or heterogeneous catalysis, a critical review. Adv Synth Catal 348:609–679. https://doi.org/10.1002/adsc.200505473

Rosa DS, Vargas BP, Silveira MV et al (2019) On the use of calcined agro-industrial waste as palladium supports in the production of eco-friendly catalysts: rice husks and banana peels tested in the Suzuki–Miyaura reaction. Waste Biomass Valori 10:2285–2296. https://doi.org/10.1007/s12649-018-0252-7

Rowland Z, Blahova A, Gao P (2022) Silver as a value keeper and wealth distributor during an economic recession. Acta Montan Slovaca 26:796–809. https://doi.org/10.46544/AMS.v26i4.16

Roy D, Uozumi Y (2018) Recent advances in palladium-catalyzed cross-coupling reactions at ppm to ppb molar catalyst loadings. Adv Synth Catal 360:602–625. https://doi.org/10.1002/adsc.201700810

Salih KSM (2022) Modern development in copper- and nickel-catalyzed cross-coupling reactions: formation of carbon-carbon and carbon-heteroatom bonds under microwave irradiation conditions. Asian J Org Chem 11:e202200023. https://doi.org/10.1002/ajoc.202200023

Schmitt CR, Duarte FA, Godoi M et al (2021) Palladium nanoparticle biosynthesis via yerba mate (*Ilex paraguariensis*) extract: an efficient eco-friendly catalyst for Suzuki–Miyaura reactions. SN Appl Sci 3:243. https://doi.org/10.1007/s42452-021-04167-6

Serrano JL, Gaware S, Pérez JA et al (2022) Quadrol-Pd (ii) complexes: phosphine-free precatalysts for the room-temperature Suzuki–Miyaura synthesis of nucleoside analogues in aqueous media. Dalton Trans 51:2370–2384. https://doi.org/10.1039/D1DT03778A

Sheikh S, Nasseri MA, Chahkandi M et al (2022) Dendritic structured palladium complexes: magnetically retrievable, highly efficient heterogeneous nanocatalyst for Suzuki and Heck cross-coupling reactions. RSC Adv 12:8833–8840. https://doi.org/10.1039/D2RA00487A

Sigma-Aldrich (2022) 216666 Tetrakis(triphenylphosphine)palladium(0) Tetrakis(triphenylphosphine)palladium(0). https://www.sigmaaldrich.com/BR/en/product/aldrich/216666. Accessed 20 Jul 2022

Su M, Huang X, Lei C, Jin J (2022) Nickel-catalyzed reductive cross-coupling of aryl bromides with vinyl acetate in dimethyl isosorbide as a sustainable solvent. Org Lett 24:354–358. https://doi.org/10.1021/acs.orglett.1c04018

Tian Y, Xing C, Wang W et al (2022) A highly crosslinked, mesoporous poly (ionic liquid) containing salen–Pd for efficient, eco-friendly Suzuki–Miyaura coupling reactions. New J Chem 46:8855–8862. https://doi.org/10.1039/D2NJ00695B

Vochozka M, Kalinova E, Gao P, Smolikova L (2021) Development of copper price from July 1959 and predicted development till the end of year 2022. Acta Montan Slovaca 26:262–280. https://doi.org/10.46544/AMS.v26i2.07

Wang Y, Liao J, Xie Z et al (2020) Zeolite-enhanced sustainable Pd-catalyzed C–C cross-coupling reaction: controlled release and capture of palladium. ACS Appl Mater Interfaces 12:11419–11427. https://doi.org/10.1021/acsami.9b18110

Wilson M, Kore R, Ritchie AW et al (2018) Palladium–poly(ionic liquid) membranes for permselective sonochemical flow catalysis. Colloid Surface A 545:78–85. https://doi.org/10.1016/j.colsurfa.2018.02.044

Wu X, Lin W, Wang L et al (2022) Highly dispersed palladium nanoclusters anchored on nanostructured hafnium(iv) oxide as highly efficient catalysts for the Suzuki–Miyaura coupling reaction. New J Chem 46:8575–8582. https://doi.org/10.1039/D2NJ00949H